

Review

# Doped Polythiophene Chiral Electrodes as Electrochemical Biosensors

M'hamed Chahma

School of Natural Sciences, Laurentian University, Sudbury, ON P3E 2C6, Canada; mchahma@laurentian.ca; Tel.: +1-705-675-1151 (ext. 2213)

**Abstract:**  $\pi$ -conducting materials such as chiral polythiophenes exhibit excellent electrochemical stability in doped and undoped states on electrode surfaces (chiral electrodes), which help tune their physical and electronic properties for a wide range of uses. To overcome the limitations of traditional surface immobilization methods, an alternative pathway for the detection of organic and bioorganic targets using chiral electrodes has been developed. Moreover, chiral electrodes have the ability to carry functionalities, which helps the immobilization and recognition of bioorganic molecules. In this review, we describe the use of polythiophenes for the design of chiral electrodes and their applications as electrochemical biosensors.

**Keywords:** polythiophenes; chirality; cyclic voltammetry; electropolymerization; sensors



**Citation:** Chahma, M. Doped Polythiophene Chiral Electrodes as Electrochemical Biosensors. *Electrochem* **2021**, *2*, 677–688. <https://doi.org/10.3390/electrochem2040042>

Academic Editor: Masato Sone

Received: 11 November 2021  
Accepted: 15 December 2021  
Published: 20 December 2021

**Publisher's Note:** MDPI stays neutral with regard to jurisdictional claims in published maps and institutional affiliations.



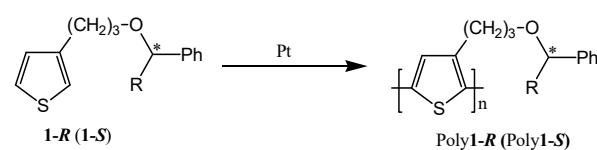
**Copyright:** © 2021 by the author. Licensee MDPI, Basel, Switzerland. This article is an open access article distributed under the terms and conditions of the Creative Commons Attribution (CC BY) license (<https://creativecommons.org/licenses/by/4.0/>).

## 1. Introduction

$\pi$ -conducting materials have emerged as excellent tools for detection of organic and bioorganic molecules, due to their stability and reversible electroactive responses [1–4]. The use of  $\pi$ -conducting materials will help overcome some of the limitations found in common methods used to modify conducting surfaces via thiols [5–7] or diazonium salts [8–10]. Moreover, their ability to amplify electrochemical signals yields the detection of low concentrations of analytes and selectively distinguishes between enantiomers. As an example, several polyaniline-based enzymatic glucose biosensors have been developed by immobilization of glucose oxidase. In addition to its high electrical conductivity and biocompatibility, polyaniline participates in electron transfer reactions allowing a facile detection of electrochemical signals resulting from the enzymatic reactions [11]. The design of other DNA electrochemical biosensors with a low limit of detection (LOD) based on conducting materials such as polypyrrole have been reported [12–14].

Owing to the presence of stereocenters on polymer backbone, chiral electrodes play an important role in several fields including biochemistry, biology and pharmacy [15–17]. The combination of biological activities with the electrochemical methods helps the differentiation of amino acid enantiomers, which may lead to the design of chiral voltammetric biosensors [18].

To the best of our knowledge, the first chiral electrode based on chiral polythiophenes was described in 1988 [19]. Chiral monothiophene monomers substituted in position 3 by either *R*(–) (1-*R*) and or *S*(+) (1-*S*) phenylbutanol were prepared and oxidized via electrochemical oxidation on platinum (Pt) electrode in nitrobenzene to form chiral electrode poly1-Pt. (Scheme 1). Both chiral electrodes (poly1-*R*-Pt and poly1-*S*-Pt) have shown stereoselectivity toward chiral doping anions.



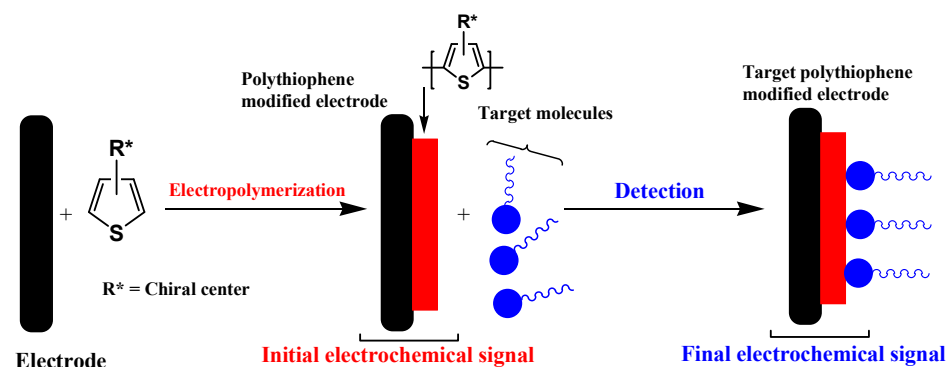
**Scheme 1.** Synthetic route of chiral electrodes poly1-*R* and poly1-*S*.

Recently, chiral electrodes based on chiral-doped polythiophenes have been found to be very efficient as spin filters at room temperature [20], which may be useful for the design of organic spin-OLED devices. Furthermore, inherently chiral electroactive electrodes display excellent chiro-optical and enantioselective properties allowing the detection of a variety of biomolecules.

Several chiral-polythiophene modified electrodes have been prepared by electropolymerization either of chiral thiophene monomers [21–23] or thiophene derivatives in the presence of chiral dopants [24–27]. Similar strategies have been employed for the preparation of chiral-polyaniline modified electrodes [28–30].

Polythiophenes are one important class of conjugated conducting materials that exhibit excellent stability at both states, reversible electrochemical responses, high conductivity and the chemistry of their precursors is well established [31–34].

Chiral electrodes based on polythiophenes can be prepared by electropolymerization of (i) either thiophene monomers bearing stereocenter at position 3 or (ii) thiophene monomers in the presence of chiral doping counter anions using cyclic voltammetry (CV). Scheme 2 displays the representation of electrochemical biosensors including the deposition of chiral polythiophenes on electrode surfaces and the recognition of selected biomolecules.

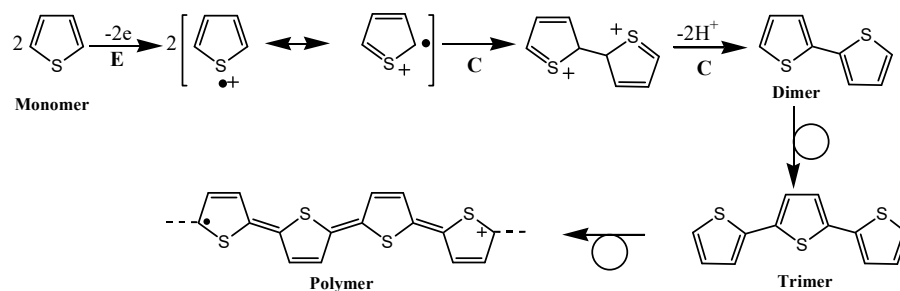


**Scheme 2.** Chiral polythiophenes as electrochemical biosensors.

Herein, we describe the design of chiral electrodes using specific thiophene derivatives and their applications as electrochemical biosensors for the detection of biomolecules in the last decade.

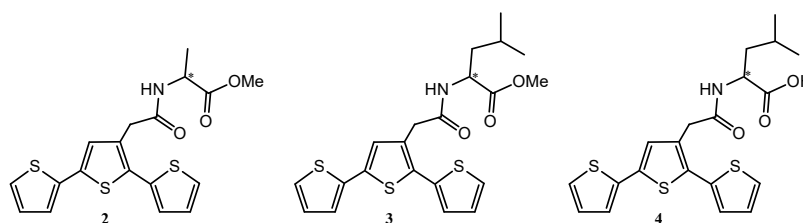
## 2. Electropolymerization

Although several chemical polymerization methods such as cross coupling reaction [35] or oxidation using  $\text{FeCl}_3$  [36] have been used to prepare polythiophene polymers, electrochemical oxidation beyond the oxidation potential of thiophene monomers on electrode surface is the method commonly used to deposit doped polythiophenes on electrode surfaces, which allows the convenient characterization of electrochemical and optical properties of the deposited films [37–39]. The electropolymerization of thiophene derivatives following an ECE mechanism [40–42] is outlined in Scheme 3. The initiation via electron transfer reaction forms a thiophene radical cation, which dimerizes after removal of two protons. The dimer will undergo similar reactions to form a trimer. The reaction chain will continue until the formation of doped polythiophenes at the surface of the electrode.



**Scheme 3.** Electropolymerization mechanism of thiophene monomers. E: Electrochemical reaction; C: Chemical reaction.

In addition to low cost, electrochemical methods display various advantages such as easy deposition/characterization of films on electrode surfaces, facile detection of target biomolecules and rapid screening results. Several monothiophenes and terthiophenes (Scheme 4) bearing chiral centers such as D-alanine (Ala) and D-leucine (Leu) have been prepared in excellent yields [43,44].



**Scheme 4.** Amino acid (AA) functionalized terthiophenes.

Due to the high oxidation potential of amino acid (AA) functionalized monothiophenes, their electropolymerization on Pt electrode were unsuccessful. On the other hand, AA functionalized terthiophenes were successfully oxidized on Pt electrode via repeated cycling CV scans.

Figure 1A shows the electropolymerization CV scans of terth-Ala-OMe (2) in ACN. The increase of the peak current confirms the successful deposition of the corresponding doped polyterthiophenes to form a chiral electrode poly2-Pt.

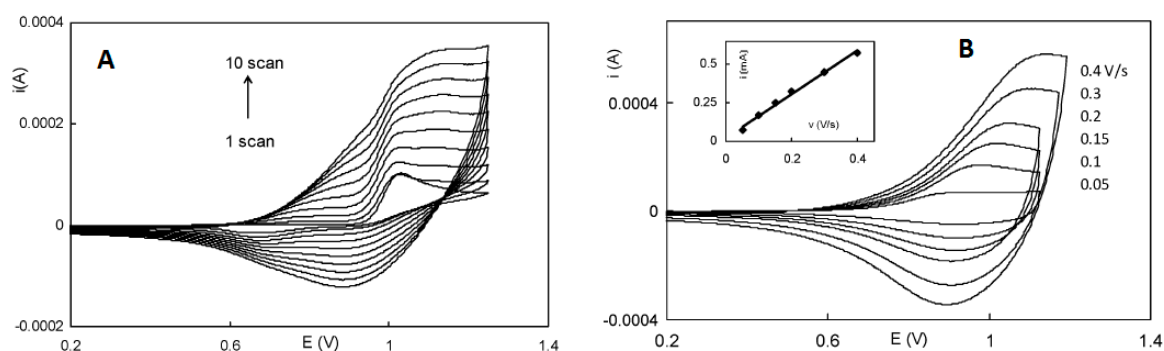


**Figure 1.** (A) The 10 scan electrochemical oxidation of terth-Ala-OMe (2) in ACN. (B) poly2-Pt at different scan rates. Reprinted with permission from reference [43]. Copyright 2010 The Royal Society of Chemistry.

In cyclic voltammetry, the examination of the relationship between the peak current with the scan rate can help to distinguish between the nature of electron transfers occurring at the surface of the electrode. For an electron transfer process controlled by diffusion species, the peak current varies linearly with the square root of a scan rate as described by the Randles–Sevcik equation (Equation (2)). On the other hand, when the electron

transfer occurs via surface-adsorbed species, the peak current varies linearly with the scan rate Equation (1).

In a free monomer solution, the peak current  $i_p$  (Figure 1B) observed for the chiral electrodes varies linearly [45,46] with the scan rate Equation (1), which indicates a surface bound species, whereas the peak current varies linearly [45,46] with square root of the scan rate Equation (2) for the diffusing redox species.

$$i_p = \frac{n^2 F^2}{4RT} \nu A \Gamma \quad (1)$$

$$i_p = 0.446 n F A C^0 \left( \frac{n F \nu D_0}{RT} \right)^{\frac{1}{2}} \quad (2)$$

$\nu$  ( $V s^{-1}$ ): scan rate;  $n$ : number of electrons;  $A$  ( $cm^2$ ): electrode surface area;  $D_0$  ( $cm^2 s^{-1}$ ): diffusion coefficient;  $C^0$  ( $mol cm^{-3}$ ): concentration of the analyte;  $\Gamma$  ( $mol cm^{-2}$ ): surface coverage.

Additionally, the peak current the chiral electrode poly2-Pt remains constant over 100 CV scans confirming the excellent stability of the chiral electrode, which is the key step in the successful detection of organic and bioorganic molecules.

### 3. Chiral Electrodes Based on Polythiophenes

Chirality has been introduced on conducting polythiophene backbones by electropolymerization of chiral precursors. Chiral electrodes based on poly3-Pt and poly4-Pt have been prepared by electropolymerization of 3 and 4 on Pt electrodes, respectively. Poly3-Pt and poly4-Pt are very stable and display excellent adhesive properties. The oxidation potential of these chiral electrodes was found to be between 0.40–0.50 V vs.  $Fc^+/Fc$ . In order to examine the sensing ability of the biosensor, the capacitive current of the chiral-poly4-Pt has been measured in the absence and presence of AA such as Ala and Leu [47]. Figure 2A shows the differences in the capacitive currents of chiral-poly4-Pt observed after addition of 1 mM of free LeuOMe. The capacitive current decreased by 30% after 30 min. Thus, the reduction of the capacitive current is due to the formation of hydrogen bonds between the free LeuOMe and the chiral-poly4-Pt layers yielding a change in the concentration of the supporting electrolyte at the interface. Moreover, the formation of the hydrogen bonds at the interface between the carboxylic acid in poly4-Pt and LeuOMe has been confirmed by  $^1H$  NMR for the monomer 4 and free LeuOMe as depicted in Figure 2C. The chemical shift of N–H (amide) group changed from 8.35 ppm to 8.50 ppm in terthiophene 4 after addition of 1 equivalent of LeuOMe and the coupling constant of the doublet (amide proton) of 4 increased from 7 Hz to 8 Hz. After 30 min, the capacitive currents of poly3-Pt remain constant after addition of 1 mM of LeuOMe (Figure 2B, control experiment), which validates the formation of hydrogen bonds on the surface of poly4-Pt.

In another study, L-Leu functionalized polyEDOT (poly5) have been synthesized in a similar fashion of poly4-Pt [48]. It was found that the chiral center was responsible for the helical structure of the poly5 backbone, and enhances the electrochemical and optical stabilities of the deposited polymer on the surface of the electrode, which is crucial for the design of chiral recognition and optical devices. Similar results have been reported for chiral polyEDOT derivatives (Scheme 5) [49].

A chiral electrode biosensor based on Ala functionalized polyEDOT for the detection of phenyl alanine and 3,4-dihydroxyphenylalanine (DOPA) have been designed by deposition on glassy carbon electrode (GCE) of poly6 [50] and poly7-R(-S) [51], respectively. CV technique was not sensitive enough to detect DOPA enantiomers by poly7-R(-S) modified GCEs. However, differential pulse voltammetry (DPV) was very effective to distinguish between D-DOPA and L-DOPA in contact with poly7-R-GCE and poly7-S-GCE as shown in Figure 3. It was found that the enantiomers D-DOPA and L-DOPA have affinities with poly7-R-GCE and poly7-S-GCE chiral electrodes, respectively. These results were consistent with results reported elsewhere [52–54].

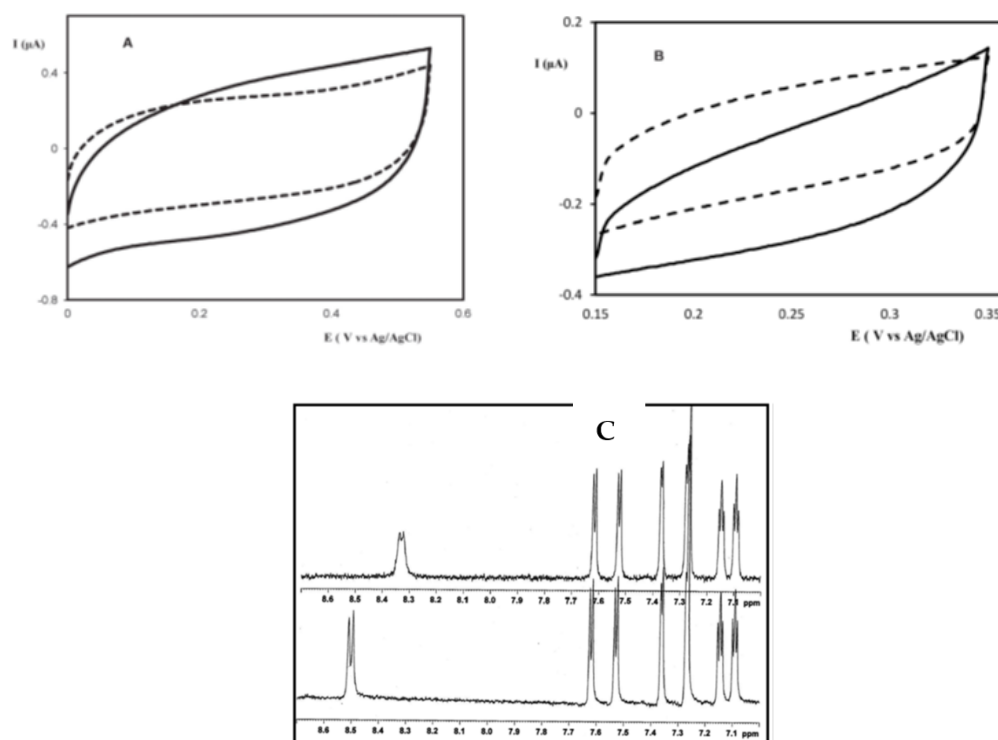
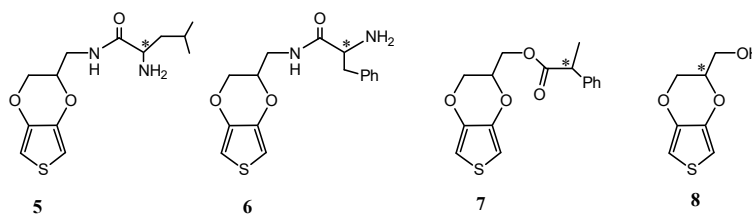


**Figure 2.** (A) Capacitive current of poly4-Pt (solid line) at concentrations 0 and 1 M of LeuOMe (dash line), (B) The capacitive current of poly3-Pt before (solid line) and after (dash line) addition of LeuOMe (1 mM), (C) <sup>1</sup>H-NMR of 1 in the absence (top) and in the presence (bottom) of one equivalent of LeuOMe. Reprinted with permission from reference [47]. Copyright 2014 The Royal Society of Chemistry.



**Scheme 5.** Chiral 3,4-ethylenedioxythiophene (EDOT) derivatives.

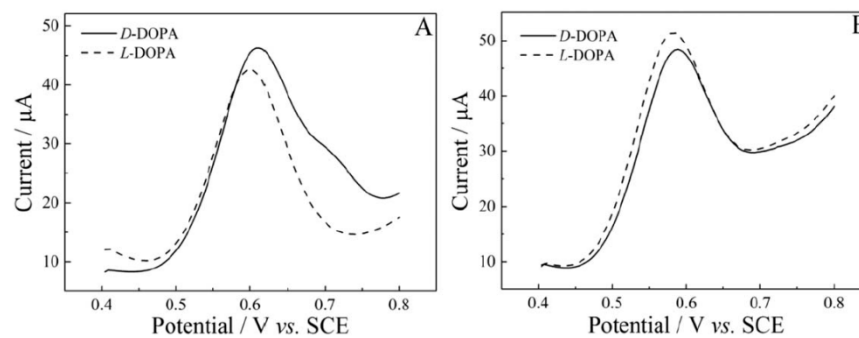
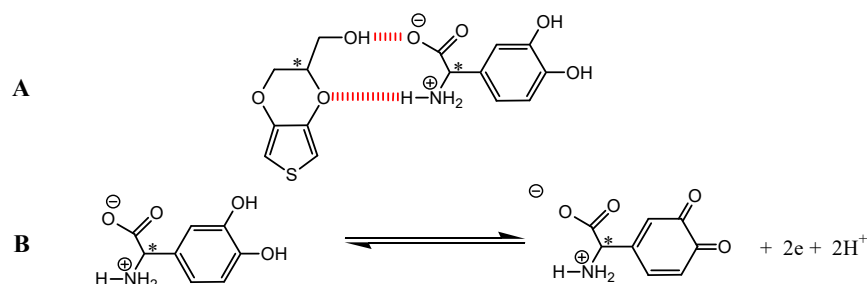


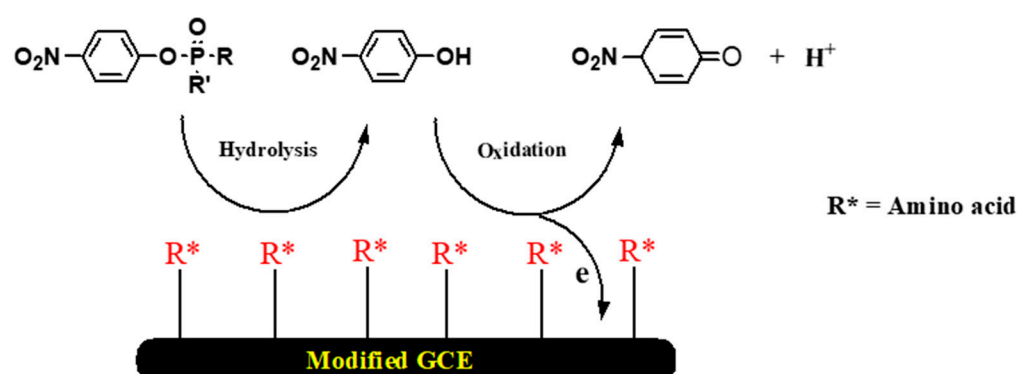
**Figure 3.** DPVs of with poly7-R-GCE (A) and poly7-S-GCE (B) modified electrodes in 0.25 M H<sub>2</sub>SO<sub>4</sub> containing 0.5 mM D-DOPA (solid line) or L-DOPA (dashed line). Reprinted with permission from reference [51]. Copyright 2015 Wiley.

Using this approach poly8-S-GCE and poly8-R-GCE chiral electrodes have been used to construct electrochemical sensors that distinguish between D-/L-DOPA, D-/L-tryptophan, and (R)-/(S)-propranolol enantiomers [55]. The mechanism of the chiral detection of these enantiomers involves the formation of hydrogen bonds between the chiral surfaces and the free DOPA (Scheme 6A), which was similar to the chiral electrode based on poly4-Pt. Moreover, the electron transfers resulting from the oxidation of hydroquinone in DOPA to quinone (Scheme 6B) amplify the electrochemical signal and thus facilitate the enantiomeric detection.



**Scheme 6.** Interaction of DOPA (A) and its oxidation (B).

An electrochemical sensor similar to natural enzyme using histidine (His), serine (Ser) and glutamic acid (Glu) functionalized polythiophene acetate acid has been employed for the detection of organophosphorus pesticides (OPs) [56]. The coexistence of three AAs on polythiophene surfaces is due to their high catalytic activity and rate of conversion for the hydrolysis of organophosphorus pesticides. Polythiophene acetate has been prepared using classical organic chemistry reaction and deposited on GCE by drop-coating with the help of 5% Nafion as a conducting adhesive binder. The three AA-polythiophenes modified GCE act as an artificial enzyme to catalyze the hydrolysis of organophosphorus pesticides yielding *p*-nitrophenol, which was further oxidized to form nitroquinone as depicted in Scheme 7. The electron/proton transfers resulting from the conversion of hydroquinone to quinone at the interface of the modified electrode/solution were measured using the square wave voltammetry (SWV), which is more sensitive than CV for the detection organophosphorus pesticides.



**Scheme 7.** Detection organophosphorus pesticides.

The AA functionalized polythiophene modified GCE has been tested for the detection of organophosphorus pesticides such as methyl paraoxon, ethyl paraoxon and methyl parathion. Figure 4 shows the current generated from the oxidation of *p*-nitrophenol to quinone measured by SWV at 1 V/s of a scan rate at an optimized pH of 5. Moreover, linear curves have been observed and the LOD was found to be lower than the value reported elsewhere [57].

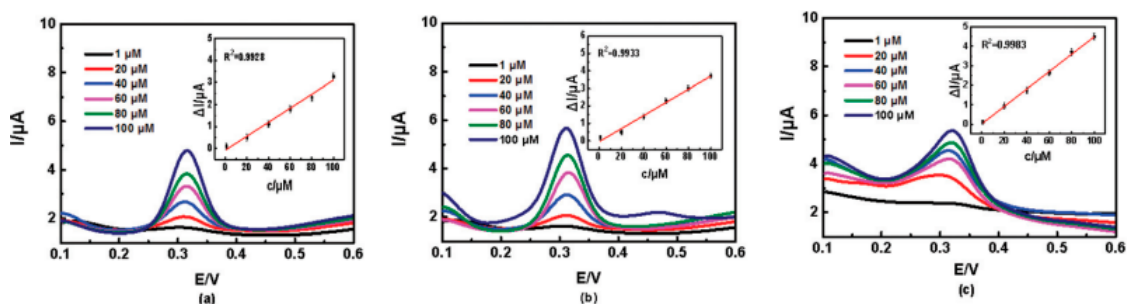


**Figure 4.** Electrochemical standard curve of the actual samples of (a) methyl paraoxon, (b) methyl parathion and (c) ethyl paraoxon with varying concentrations. Reprinted with permission from reference [56]. Copyright 2020 The Royal Society of Chemistry.

Another approach to introduce chirality on polythiophenes via molecularly imprinted polymers (MIPs) has been reported [58]. MIPs were deposited onto Au QCM (quartz crystal microbalance) electrode surface via CV scans in ACN of terthiophene carboxylic acid in the presence of (–)-norephedrine (Figure 5a). Figure 5b displays the frequency changes observed during the electropolymerization process from doped to undoped polyterthiophenes. In order to confirm the successful incorporation of the chiral motifs by polyterthiophene films, MIPs have been characterized by XPS technique, which shows binding energy features of polyterthiophenes (strong sulfur 2p doublet between 163 and 166 eV) and of (–)-norephedrine motifs (nitrogen 2s peak between 399 and 403 eV).

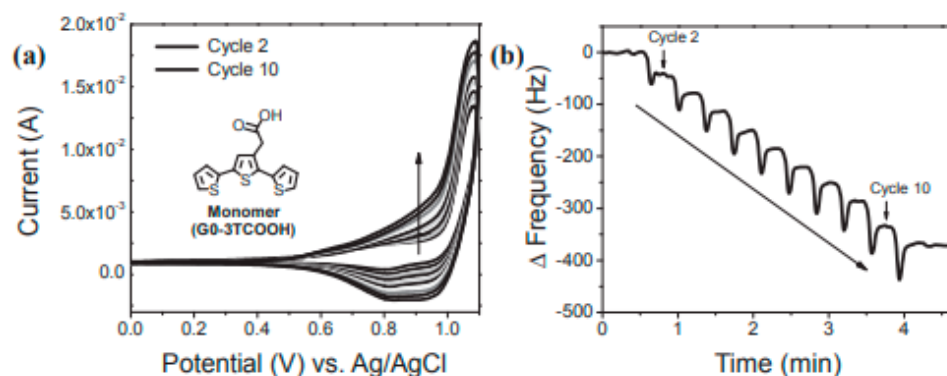


**Figure 5.** EC-QCM in situ measurements of the CV electrodeposition of the MIP film onto PS- (500 nm size) templated Au surface: (a) CV diagram and (b) QCM response. Reprinted with permission from reference [58]. Copyright 2012 Wiley.

After characterization of the (–)-norephedrine nanostructured MIP surface, the MIP-QCM sensor has been tested for the distinction between (–)-norephedrine (1R, 2S) and its diastereomer (+)-norephedrine (1S, 2S). A change in the frequency response of the (–)-norephedrine imprinted MIP QCM sensor in contact with (–)-norephedrine has been observed in Figure 6a. However, no significant change of the frequency of the MIP QCM sensor in contact with the antagonist (+)-norephedrine has been noticed. Similar tendency has been perceived with less frequency response for of (+)-norephedrine nanostructured MIP sensor in contact with (+)-norephedrine.

Moreover, the frequency response of the nanostructured MIP-QCM sensor follows a linear response with the concentration of the target norephedrine. Other polypyrrole-MIPs based on MOF-5 derived porous carbon nanotube and Prussian blue nanocube sensors have been used to distinguish between cysteine enantiomers [59].

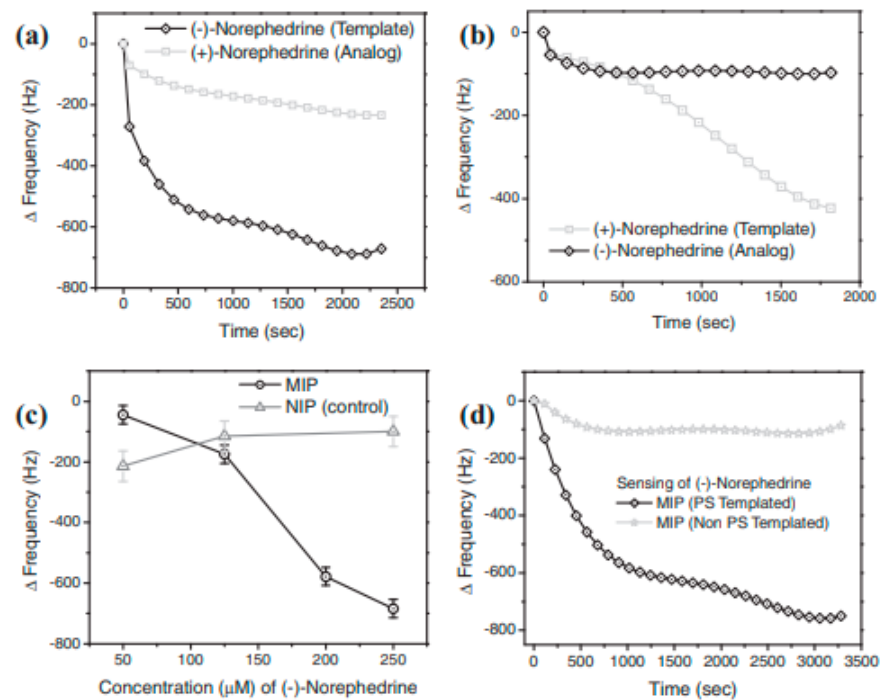


**Figure 6.** QCM sensing of 250  $\mu$ M concentration of (a) (–)-norephedrine, (b) (+)-norephedrine, (c) (–)-norephedrine sensing calibration plot of the MIP film versus the NIP (control) and (d) comparison of the sensing response of the PS and non-PS-templated MIP film. Reprinted with permission from reference [58]. Copyright 2012 Wiley.

Using nanoparticles, another method has been developed to introduce chirality on polythiophene surfaces as shown in Figure 7 (left) [60]. After deposition of polythiophenes on GCE via electropolymerization process,  $\text{MnO}_2$  nanoparticles have also been deposited following a similar procedure described for polyEDOT using  $\text{KMnO}_4$  [61] to form  $\text{MnO}_2$ -NPs/PolyTh/GCE surface. Then, the D-amino acid oxidase (DAAO) and hemoglobin (Hb) were immobilized on the surface via electrostatic interactions to form DAAO-Hb/ $\text{MnO}_2$ -NPs/PolyTh/GCE sensor. Redox peaks of dopamine (anodic peak at 0.17 V and cathodic peak at 0.11 V) have been observed on DAAO-Hb/ $\text{MnO}_2$ -NPs/PolyTh/GCE sensor (Figure 7 right), but these peaks are absent in other surfaces certifying the excellent selectivity of this sensor toward the detection of dopamine motifs.

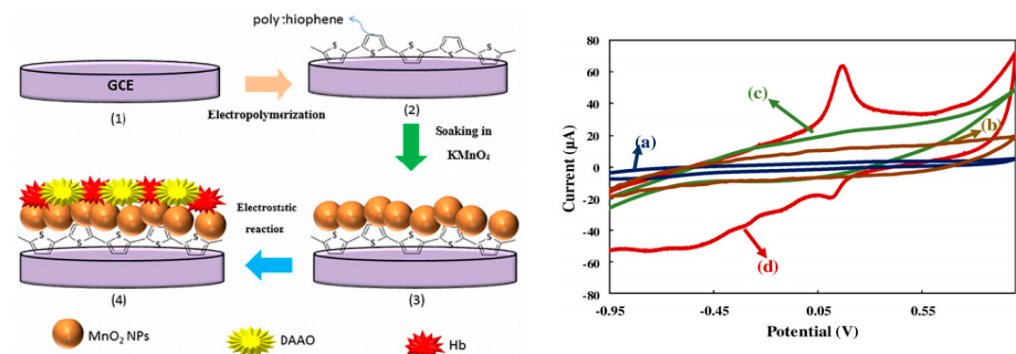


**Figure 7.** Left: Fabrication steps of the DAAO-Hb/ $\text{MnO}_2$  NPs/PTTh/GCE bi-enzyme biosensor. Right: CVs of (a) bare GCE, (b) PTh/GCE, (c)  $\text{MnO}_2$  NPs/PTTh/GCE and (d) DAAO-Hb/ $\text{MnO}_2$  NPs/PTTh/GCE in PBS solution (100 mM, pH = 6) containing 200  $\mu$ M D-alanine and 5  $\mu$ M DAAO at scan rate of 100 mV/s. Reprinted with permission from reference [60]. Copyright 2017 Elsevier.

Dopamine enantiomers have been differentiated by second-derivative linear sweep voltammetry (SDLSV) using MnO<sub>2</sub>/nitrogen-doped graphene nanocomposites sensor [62]. In this method, the LOD was found to be 0.039 μM whereas the LOD was found to be 40 nM using DAAO-Hb/MnO<sub>2</sub> NPs/PTh/GCE sensor, which validates the importance of polythiophenes for amplifying the sensitivity of electrochemical signals to lower limits of detection.

#### 4. Concluding Remarks

Efforts have been made to design chiral electrodes for the detection of a variety of biomolecules. Taking advantage of the well-established electrochemical properties of polythiophenes, the facile use and low cost of electrochemical methods such as CV and DPV, distinction between enantiomers has been made possible by amplifying the electrochemical signals. Table 1 summarizes a few electrochemical biosensors using polythiophene chiral electrodes.

**Table 1.** Examples of electrochemical chiral electrode sensors.

Electrode Construction	Detection	LOD	Ref
Leu/PTh/Pt	LeuOMe/AlaOMe	1 mM	[47]
PTh/GCE	1,4-Dihydroxyphenylalanine	0.50 mM	[51]
Norephedrine/PTh/QCM	Norephedrine	0.25 mM	[58]
His-Ser-Glu/PTh/GCE	Organophosphorus	0.50 μM	[56]
DAAO-Hb/MnO <sub>2</sub> NPs/PTh/GCE	Dopamine	40 nM	[60]
DAAO-Hb/MnO <sub>2</sub> NPs/GCE	Dopamine	0.039 μM	[62]
PPy-DEX/GR/GCE	Mandelic acid	0.25 mM	[63]
Trp/PPy/Au	L-Tryptophan, D-Tryptophan	0.012 μM, 0.009 μM	[64]
L/D-CNT/PPy/Pt	Amino acids (Tryptophan)	0.107 nM	[65]
PANi/GCE	L-Glutamic acid	0.011 mM	[66]
PANI-FSA/PGE	L-Ascorbic acid	7.3–4.5 10 <sup>-4</sup> nM	[67]
L-Cys-Au/Fe <sub>3</sub> O <sub>4</sub> -NP	L-and D-Tyrosine	0.021–0.084 μM	[68]
GCE	L-Tyrosine, D-Tyrosine	0.65, 0.86 mM	[69]
Cu-β-CD/PLA/MWCN/GCE.	Tryptophan	3.3 10 <sup>-7</sup> M	[70]

Chiral electrodes based on polythiophenes exhibit similar LOD observed for chiral -polypyrroles and -polyanilines modified electrodes. However, they present better LOD than traditional chiral electrodes, which may be explained by the amplification of the electrical signal resulting from the conducting materials and the diminution of the signal noise.

Chiral electrode sensors are very effective and can be used as an alternative to traditional methods utilized to modify conducting surfaces and detect biomolecules. However, the design of chiral electrodes using new chiral polythiophenes that are very stable on the surface of the electrodes and chiro-selective toward target are important challenges for successful electrochemical biosensors.

**Funding:** This research received no external funding.

**Institutional Review Board Statement:** Not Applicable.

**Informed Consent Statement:** Not Applicable.

**Data Availability Statement:** Not Applicable.

**Acknowledgments:** We thank Laurentian University.

**Conflicts of Interest:** The authors declare no conflict of interest.

## References

1. Terán-Alcocer, A.; Bravo-Plascencia, F.; Cevallos-Morillo, C.; Palma-Cando, A. Electrochemical sensors based on conducting polymers for the aqueous detection of biologically relevant molecules. *Nanomaterials* **2021**, *11*, 252. [[CrossRef](#)] [[PubMed](#)]
2. Arnaboldi, S.; Grecchi, S.; Magni, M.; Mussini, P. Electroactive chiral oligo- and polymer layers for electrochemical enantioselective recognition. *Curr. Opin. Electrochem.* **2018**, *7*, 188–199. [[CrossRef](#)]
3. Chahma, M.; Gilroy, J.B.; Hicks, R.G. Linear and branched electroactive polymers based on ethylenedioxythiophene–triarylamine conjugates. *J. Mater. Chem.* **2007**, *17*, 4768–4771. [[CrossRef](#)]
4. Ibanez, J.G.; Rincon, M.E.; Gutierrez-Granados, S.; Chahma, M.; Jaramillo-Quintero, O.A.; Frontana-Urbe, B.A. Conducting polymers in the fields of energy, environmental remediation, and chemical–chiral sensors. *Chem. Rev.* **2018**, *118*, 4731–4816.
5. Mandler, D. Chiral self-assembled monolayers in electrochemistry. *Curr. Opin. Electrochem.* **2018**, *7*, 42–47. [[CrossRef](#)]
6. Chahma, M.; Lee, J.S.; Kraatz, H.-B. Fc-ssDNA conjugate: Electrochemical properties in a borate buffer and adsorption on gold electrode surfaces. *J. Electroanal. Chem.* **2004**, *567*, 283–287. [[CrossRef](#)]
7. Vericat, C.; Vela, M.E.; Benitez, G.; Carro, P.; Salvarezza, R.C. Self-assembled monolayers of thiols and dithiols on gold: New challenges for a well-known system. *Chem. Soc. Rev.* **2010**, *39*, 1805–1834. [[CrossRef](#)] [[PubMed](#)]
8. Combellas, C.; Kanoufi, F.; Pinson, J.; Podvorica, F.I. Sterically hindered diazonium salts for the grafting of a monolayer on metals. *J. Am. Chem. Soc.* **2008**, *130*, 8576–8577. [[CrossRef](#)]
9. Adenier, A.; Combellas, C.; Kanoufi, F.; Pinson, J.; Podvorica, F.I. Formation of polyphenylene films on metal electrodes by electrochemical reduction of benzenediazonium salts. *Chem. Mater.* **2006**, *18*, 2021–2029. [[CrossRef](#)]
10. Assresahegn, B.D.; Brousse, T.; Bélanger, D. Advances on the use of diazonium chemistry for functionalization of materials used in energy storage systems. *Carbon* **2015**, *92*, 362–381. [[CrossRef](#)]
11. Lai, J.; Yi, Y.; Zhu, P.; Shen, J.; Wu, K.; Zhang, L.; Liu, J. Polyaniline-based glucose biosensor: A review. *J. Electroanal. Chem.* **2016**, *782*, 138–153. [[CrossRef](#)]
12. Thompson, L.A.; Kowalik, J.; Josowicz, M.; Janata, J. Label-free DNA hybridization probe based on a conducting polymer. *J. Am. Chem. Soc.* **2003**, *125*, 324–325. [[CrossRef](#)] [[PubMed](#)]
13. Lakard, B. Electrochemical biosensors based on conducting polymers: A review. *Appl. Sci.* **2020**, *10*, 6614. [[CrossRef](#)]
14. Saheb, A.; Patterson, S.; Josowicz, M. Probing for DNA methylation with a voltammetric DNA detector. *Analyst* **2014**, *139*, 786–792. [[CrossRef](#)]
15. Arnaboldi, S.; Magni, M.; Mussini, P.R. Enantioselective selectors for chiral electrochemistry and electroanalysis: Stereogenic elements and enantioselective performance. *Curr. Opin. Electrochem.* **2018**, *8*, 60–72. [[CrossRef](#)]
16. Kane-Maguire, L.A.P.; Wallace, G.G. Chiral conducting polymers. *Chem. Soc. Rev.* **2010**, *39*, 2545–2576. [[CrossRef](#)]
17. Vacek, J.; Zadny, J.; Storch, J.; Hrbac, J. Chiral electrochemistry: Anodic deposition of enantiopure helical molecules. *ChemPlusChem* **2020**, *85*, 1954–1958. [[CrossRef](#)] [[PubMed](#)]
18. Trojanowicz, M. Enantioselective electrochemical sensors and biosensors: A mini-review. *Electrochem. Commun.* **2014**, *38*, 47–52. [[CrossRef](#)]
19. Lemaire, M.; Delabouglise, D.; Garreau, R.; Guy, A.; Roncali, J. Enantioselective chiral poly(thiophenes). *Chem. Commun.* **1988**, *10*, 658–661. [[CrossRef](#)]
20. Mondal, P.C.; Kantor-Uriel, N.; Mathew, S.P.; Tassinari, F.; Fontanesi, C. Chiral conductive polymers as spin filters. *Adv. Mater.* **2015**, *27*, 1924–1927. [[CrossRef](#)]
21. Salmón, M.; Bidan, G. Chiral polypyrroles from optically active pyrrole monomers. *J. Electrochem. Soc.* **1985**, *132*, 1897–1899. [[CrossRef](#)]
22. Ramos, J.C.; Dias, J.M.M.; Souto-Maior, R.M.; Ribeiro, A.S.; Tonholo, J.; Barbier, V.; Penelle, J.; Navarro, M. Synthesis and characterization of poly[(R)-(–) and (S)-(+)-3-(1'-pyrrolyl)propyl-N-(3'',5''-dinitrobenzoyl)- $\alpha$ -phenylglycinate]s as chiral oligomers of pyrrole. *Synth. Met.* **2010**, *160*, 1920–1924. [[CrossRef](#)]
23. Takano, N.; Seki, C. Preparation of chiral polypyrrole film-coated electrode incorporating palladium metal and asymmetric hydrogenation of  $\alpha$ -keto esters. *Electrochemistry* **2006**, *74*, 596–598. [[CrossRef](#)]
24. Deore, B.; Yakabe, H.; Shiigi, H.; Nagaok, T. Enantioselective uptake of amino acids using an electromodulated column packed with carbon fibres modified with overoxidised polypyrrole. *Analyst* **2002**, *127*, 935–939. [[CrossRef](#)] [[PubMed](#)]
25. Syritski, V.; Reut, J.; Menaker, A.; Gyurcsányi, R.E.; Öpik, A. Electrosynthesized molecularly imprinted polypyrrole films for enantioselective recognition of L-aspartic acid. *Electrochim. Acta* **2008**, *53*, 2729–2736. [[CrossRef](#)]
26. Yang, J.; Yu, Y.; Wu, D.; Tao, Y.; Deng, L.; Kong, Y. Coinduction of a chiral microenvironment in polypyrrole by overoxidation and camphorsulfonic acid for electrochemical chirality sensing. *Anal. Chem.* **2018**, *90*, 9551–9558. [[CrossRef](#)]
27. Zhao, Q.; Yang, J.; Zhang, J.; Wu, D.; Tao, Y.; Kong, Y. Single-template molecularly imprinted chiral sensor for simultaneous recognition of alanine and tyrosine enantiomers. *Anal. Chem.* **2019**, *91*, 12546–12552. [[CrossRef](#)] [[PubMed](#)]
28. Basozabal, I.; Gómez-Caballero, A.; Unceta, N.; Goicolea, M.A.; Barrio, R.J. Voltammetric sensors with chiral recognition capability: The use of a chiral inducing agent in polyaniline electrochemical synthesis for the specific recognition of the enantiomers of the pesticide dinoseb. *Electrochim. Acta* **2011**, *58*, 729–735. [[CrossRef](#)]
29. He, S.; Shang, X.; Lu, W.; Tian, Y.; Xu, Z.; Zhang, W. Electrochemical enantioselective sensor for effective recognition of tryptophan isomers based on chiral polyaniline twisted nanoribbon. *Anal. Chim. Acta* **2021**, *1147*, 155–164. [[CrossRef](#)]

30. Feng, Z.; Li, M.; Yan, Y.; Jihai, T.; Xiao, L.; Wei, Q. Several novel and effective methods for chiral polyaniline to recognize the configuration of alanine. *Tetrahedron Asymmetry* **2012**, *23*, 411–414. [[CrossRef](#)]
31. Tourillon, G.; Garnier, F. Stability of conducting polythiophene and derivatives. *J. Electrochem. Soc.* **1983**, *130*, 2042–2044. [[CrossRef](#)]
32. Joergensen, M.; Norrman, K.; Gevorgyan, S.A.; Tromholt, T.; Andreasen, B.; Krebs, F.C. Stability of Polymer Solar Cells. *Adv. Mater.* **2012**, *24*, 580–612. [[CrossRef](#)] [[PubMed](#)]
33. So, R.C.; Carreon-Asok, A.C. Molecular design, synthetic strategies, and applications of cationic polythiophenes. *Chem. Rev.* **2019**, *119*, 11442–11509. [[CrossRef](#)]
34. Kaloni, T.P.; Giesbrecht, P.K.; Schreckenbach, G.; Freund, M.S. Polythiophene: From fundamental perspectives to applications. *Chem. Mater.* **2017**, *29*, 10248–10283. [[CrossRef](#)]
35. Yamamoto, T.; Koizumi, T.A. Synthesis of  $\pi$ -conjugated polymers bearing electronic and optical functionalities by organometallic polycondensations and their chemical properties. *Polymer* **2007**, *48*, 5449–5472. [[CrossRef](#)]
36. Nilsson, K.P.R.; Johan, D.; Olsson, J.D.; Konradsson, P.; Inganas, O. Enantiomeric substituents determine the chirality of luminescent conjugated polythiophenes. *Macromolecules* **2004**, *37*, 6316–6321. [[CrossRef](#)]
37. Chahma, M.; Myles, D.J.T.; Hicks, R.G. Synthesis and characterization of a conducting organomain group polymer, poly[bis((3,4-ethylenedioxy)-2-thienyl) sulfide]: A heteroaromatic relative of poly(p-phenylene sulfide). *Macromolecules* **2004**, *37*, 2010–2012. [[CrossRef](#)]
38. Roncali, J. Conjugated poly (thiophenes): Synthesis, functionalization, and applications. *Chem. Rev.* **1992**, *92*, 711–738. [[CrossRef](#)]
39. Groenendaal, L.; Jonas, F.; Freitag, D.; Pielartzik, H.; Reynolds, J.R. Poly(3, 4-ethylenedioxythiophene) and its derivatives: Past, present, and future. *Adv. Mater.* **2000**, *12*, 481–534. [[CrossRef](#)]
40. Genies, E.M.; Bidan, G.; Diaz, A.F. Spectroelectrochemical study of polypyrrole films. *J. Electroanal. Chem.* **1983**, *149*, 101–113. [[CrossRef](#)]
41. Amatore, C.; Savéant, J.-M. ECE and disproportionation: Part, V. Stationary state general solution application to linear sweep voltammetry. *J. Electroanal. Chem.* **1977**, *85*, 27–46.
42. Andrieux, C.P.; Audebert, P.; Hapiot, P.; Savéant, J.-M. Identification of the first steps of the electrochemical polymerization of pyrroles by means of fast potential step techniques. *J. Phys. Chem.* **1991**, *95*, 10158–10164. [[CrossRef](#)]
43. McTiernan, C.D.; Chahma, M. Synthesis and characterization of alanine functionalized oligo/polythiophenes. *New J. Chem.* **2010**, *34*, 1417–1423. [[CrossRef](#)]
44. McTiernan, C.D.; Omri, K.; Chahma, M. Chiral conducting surfaces via electrochemical oxidation of L-leucine-oligothiophenes. *J. Org. Chem.* **2010**, *75*, 6096–6103. [[CrossRef](#)] [[PubMed](#)]
45. Elgrishi, N.; Rountree, K.J.; McCarthy, B.D.; Rountree, E.S.; Eisenhart, T.T.; Dempsey, J.L. A practical beginner's guide to cyclic voltammetry. *J. Chem. Educ.* **2018**, *95*, 197–206. [[CrossRef](#)]
46. Bard, A.J.; Faulkner, L.R. *Electrochemical Methods. Fundamentals and Applications*, 2nd ed.; Wiley: New York, NY, USA, 2001.
47. Chahma, M.; McTiernan, C.D.; Abbas, S.A. Characterization of phenomena occurring at the interface of chiral conducting surfaces. *New J. Chem.* **2014**, *38*, 3379–3385. [[CrossRef](#)]
48. Hu, D.; Lu, B.; Duan, X.; Xu, J.; Zhang, L.; Zhang, K.; Zhang, S.; Zhen, S. Synthesis of novel chiral l-leucine grafted PEDOT derivatives with excellent electrochromic performances. *RSC Adv.* **2014**, *4*, 35597–35608. [[CrossRef](#)]
49. Grenier, R.G.; George, S.J.; Joncheray, T.J.; Meijer, E.W.; Reynolds, J.R. Chiral ethylhexyl substituents for optically active aggregates of  $\pi$ -conjugated polymers. *J. Am. Chem. Soc.* **2007**, *129*, 10694–10699. [[CrossRef](#)] [[PubMed](#)]
50. Hu, D.; Lu, B.; Zhang, K.; Sun, X.; Xu, J.; Duan, X.; Dong, L.; Sun, H.; Zhu, X.; Zhen, S. Synthesis of novel chiral L-phenylalanine grafted PEDOT derivatives with electrochemical chiral sensor for 3,4-dihydroxyphenylalanine discrimination. *Int. J. Electrochem. Sci.* **2015**, *10*, 3065–3081.
51. Dong, L.; Lu, B.; Duan, X.; Xu, J.; Hu, D.; Zhang, K.; Zhu, X.; Sun, H.; Ming, S.; Wang, Z.; et al. Novel chiral PEDOTs for selective recognition of 3, 4-dihydroxyphenylalanine enantiomers: Synthesis and characterization. *J. Polym. Sci. Part A Polym. Chem.* **2015**, *53*, 2238–2251. [[CrossRef](#)]
52. Dong, L.; Zhang, Y.; Duan, X.; Zhu, X.; Su, H.; Xu, J. Chiral PEDOT-based enantioselective electrode modification material for chiral electrochemical sensing: Mechanism and model of chiral recognition. *Anal. Chem.* **2017**, *89*, 9695–9702. [[CrossRef](#)]
53. Arnaboldi, S.; Benincori, T.; Cirilli, R.; Grecchi, S.; Santagostini, L.; Sannicolò, F.; Mussini, P.R. "Inherently chiral" thiophene-based electrodes at work: A screening of enantioselection ability toward a series of pharmaceutically relevant phenolic or catecholic amino acids, amino esters, and amine. *Anal. Bioanal. Chem.* **2016**, *408*, 7243–7254. [[CrossRef](#)] [[PubMed](#)]
54. Arnaboldi, S.; Benincori, T.; Cirilli, R.; Kutner, W.; Magni, M.; Mussini, P.R.; Noworyta, K.; Sannicolò, F. Inherently chiral electrodes: The tool for chiral voltammetry. *Chem. Sci.* **2015**, *6*, 1706–1711. [[CrossRef](#)] [[PubMed](#)]
55. Wattanakit, C.; Côme, Y.; Lapeyre, V.; Bopp, P.A.; Heim, M.; Yadnum, S.; Nokbin, S.; Warakulwit, C.; Limtrakul, J.; Kuhn, A. Enantioselective recognition at mesoporous chiral metal surfaces. *Nat. Commun.* **2014**, *5*, 3325. [[CrossRef](#)]
56. Liu, Y.; Cao, X.; Liu, Z.; Sun, L.; Fang, G.; Liu, J.; Wang, S. Electrochemical detection of organophosphorus pesticides based on amino acids-conjugated P3TAA-modified electrodes. *Analyst* **2020**, *145*, 8068–8076. [[CrossRef](#)] [[PubMed](#)]
57. Xu, M.-L.; Gao, Y.; Han, X.X.; Zhao, B. Detection of pesticide residues in food using surface-enhanced Raman spectroscopy: A review. *J. Agric. Food Chem.* **2017**, *65*, 6719–6726. [[CrossRef](#)] [[PubMed](#)]

58. Pernites, R.B.; Venkata, S.K.; Tiu, B.D.B.; Yago, A.C.C.; Advincula, R.C. Nanostructured, molecularly imprinted, and template-patterned polythiophenes for chiral sensing and differentiation. *Small* **2012**, *8*, 1669–1674. [[CrossRef](#)] [[PubMed](#)]
59. Duan, D.; Yang, H.; Ding, Y.; Li, L.; Ma, G. A three-dimensional conductive molecularly imprinted electrochemical sensor based on MOF derived porous carbon/carbon nanotubes composites and prussian blue nanocubes mediated amplification for chiral analysis of cysteine enantiomers. *Electrochim. Acta* **2019**, *302*, 137–144. [[CrossRef](#)]
60. Shoja, Y.; Rafati, A.A.; Ghodsi, J. Polythiophene supported MnO<sub>2</sub> nanoparticles as nano-stabilizer for simultaneously electrostatically immobilization of d-amino acid oxidase and hemoglobin as efficient bio-nanocomposite in fabrication of dopamine bi-enzyme biosensor. *Mater. Sci. Eng. C* **2017**, *76*, 637–645. [[CrossRef](#)] [[PubMed](#)]
61. Liu, R.; Duay, J.; Lee, S.B. Redox exchange induced MnO<sub>2</sub> nanoparticle enrichment in poly(3,4-ethylenedioxythiophene) nanowires for electrochemical energy storage. *ACS Nano* **2010**, *4*, 4299–4307. [[CrossRef](#)]
62. Li, Q.; Xia, Y.; Wan, X.; Yang, S.; Cai, Z.; Ye, Y.; Li, G. Morphology-dependent MnO<sub>2</sub>/nitrogen-doped graphene nanocomposites for simultaneous detection of trace dopamine and uric acid. *Mater. Sci. Eng. C* **2020**, *109*, 110615. [[CrossRef](#)] [[PubMed](#)]
63. Borazjani, M.; Mehdinia, A.; Jabbari, A. An enantioselective electrochemical sensor for simultaneous determination of mandelic acid enantiomers using dexamethasone-based chiral nanocomposite coupled with chemometrics method. *J. Electroanal. Chem.* **2017**, *805*, 83–90. [[CrossRef](#)]
64. Niu, X.; Yang, X.; Mo, Z.; Pan, Z.; Liu, Z.; Shuai, C.; Gao, Q.; Liu, N.; Guo, R. Electrochemical chiral recognition at molecular imprinting Au surfaces. *J. Electrochem. Soc.* **2019**, *166*, B1126–B1130. [[CrossRef](#)]
65. Ning, G.; Wang, H.; Fu, M.; Liu, J.; Sun, Y.; Lu, H.; Fan, X.; Zhang, Y.; Wang, H. Dual signals electrochemical biosensor for point-of-care testing of amino acids enantiomers. *Electroanalysis* **2021**. [[CrossRef](#)]
66. Zeng, X.; Li, N.; Wang, J. Electrochemical synthesis of (poly) dimethoxyaniline on glassy carbon electrodes and their applications in the detection of L and D-glutamic acids. *J. Electrochem. Soc.* **2019**, *166*, B3066–B3071. [[CrossRef](#)]
67. Pandey, I.; Kant, R. Electrochemical impedance based chiral analysis of anti-ascorbic drug: L-Ascorbic acid and d-ascorbic acid using C-dots decorated conductive polymer nano-composite electrode. *Biosens. Bioelectron.* **2016**, *77*, 715–724. [[CrossRef](#)]
68. Shi, X.; Wang, Y.; Peng, C.; Zhang, Z.; Chen, J.; Zhou, X.; Jiang, H. Enantiorecognition of tyrosine based on a novel magnetic electrochemical chiral sensor. *Electrochim. Acta* **2017**, *241*, 386–394. [[CrossRef](#)]
69. Zou, J.; Yu, J.G. Chiral recognition of tyrosine enantiomers on a novel bis-aminosaccharides composite modified glassy carbon electrode. *Anal. Chim. Acta* **2019**, *1088*, 35–44. [[CrossRef](#)] [[PubMed](#)]
70. Lei, P.; Zhou, Y.; Zhang, G.; Zhang, Y.; Zhang, C.; Hong, S.; Yang, Y.; Dong, C.; Shuang, S. A highly efficient chiral sensing platform for tryptophan isomers based on a coordination self-assembly. *Talanta* **2019**, *195*, 306–312. [[CrossRef](#)] [[PubMed](#)]